보건학석사 학위논문

Octanol–water distribution coefficients of fungal particles collected from the atmosphere

대기 중 부유 진균의 옥탄올–물 분배계수 연구

2018 년 2 월

서울대학교 보건대학원

환경보건학과 환경보건학 전공

우 철 운

Octanol–water distribution coefficients of fungal particles collected from the atmosphere

대기 중 부유 진균의 옥탄올–물 분배계수 연구

지도교수 Naomichi Yamamoto

이 논문을 보건학석사 학위 논문으로 제출함

2017 년 11 월

서울대학교 보건대학원

훤경보건학과 환경보건학 전공

우 철 운

우철운의 보건학석사 학위논문을 인준함

2017 년 12 월

위 원 장 이 승 묵 (인)

부 위 원 장 김 성 균 (인)

위 원 Naomichi Yamamoto (인)

Abstract

Octanol–water distribution coefficients of fungal particles collected from the atmosphere

Cheolwoon Woo

Department of Environmental Health

Graduate School of Public Health, Seoul National University

Fungi are well-known spore-producing organisms that secrete particles of various shapes, sizes, surface properties, and other features to adapt to different environments. The released fungal particles, including spores, hyphae, and fragments, can act as ice nuclei and/or cloud condensation nuclei and actively participate in local and global hydrological cycles. The degree of hydrophobicity of fungal particle surfaces might play an important role in their ability to act as the ice nuclei or cloud condensation nuclei. Therefore, in this study, we employ the octanol–water distribution coefficient to identify the degree of hydrophobicity of the fungal particles collected from the atmosphere in Seoul, South Korea. The airborne fungal particles were collected from the atmosphere using a two-stage cyclone sampler. The collected fungal particles were classified based on their surface properties using the frozen water phase method. The

taxon-specific octanol–water distribution coefficients of the fungal particles were determined by quantifying every taxon in each phase using the combination of quantitative PCR and high-throughput sequencing methods. The octanol–water distribution coefficients of Ascomycota and Basidiomycota, which are considered as the predominant phyla of fungi, were not statistically different across the sampling period. Additionally, the octanol–water distribution coefficients of the two phyla showed similar patterns of variation, which had been affected by sampling period. Moreover, the octanol–water distribution coefficients at genus rank showed a high variability across the sampling period. Hierarchical cluster analysis revealed that the fungal genera were not taxonomically grouped by the octanol–water distribution coefficients of each fungal genus. Spearman's correlation analysis and generalized linear model demonstrated the potential possibility that some environmental factors, climatological condition, and concentration of anthropogenic air pollutants measured weekly could modify the fungal particle surface and change the degree of octanol–water distribution coefficients. The result of this study revealed that the degree of hydrophobicity of fungal particles could vary according to species. In addition, the degree of hydrophobicity of fungal particles might be affected by the ambient air pollutants, which is likely influenced by the concentration of air pollutants and the residence time of fungal particles in the atmosphere. Consequently, we expect that ice nucleation and cloud condensation nucleation activity of fungal particles could vary depending on the fungal species and residence time of fungal particles in the atmosphere.

Keywords: Octanol–water distribution coefficient, Airborne fungal particles, Degree of hydrophobicity, Surface property, Ice nuclei, Cloud condensation nuclei

Student number: 2016-24051

Contents

List of Figures

List of Tables

1. Introduction

Fungi are well-known spore-producing organisms, and 1.5 million species are estimated to exist (Hawksworth, 2001). They produce spores of various shapes, sizes, surface properties, and other features to adapt to different environments. Fungal materials such as spores, hyphae, and fragments are released into the atmosphere at 28–50 Tg/year (Heald et al., 2009 and Elbert et al., 2007). Furthermore, the released fungal particles can act as ice nuclei (IN) and/or cloud condensation nuclei (CCN) and actively participate in local and global hydrological cycles (Fröhlich-Nowoisky et al., 2016). For instance, fungal particles with diameters larger than 2 μm can serve as giant CCN (GCCN) and have important roles in cloud formation via water condensation (Möhler et al., 2007). Hassett et al. (2015) hypothesized that the degree of hydrophobicity of fungal spore surface might play an important role in the hydrological cycle.

However, the degree of hydrophobicity of fungal spore surface remains poorly understood. The fungal spore surfaces are composed of various components. Among these components, hydrophobins and mannitol seem to influence the degree of hydrophobicity of fungal spore surface. Hydrophobins are surface active proteins that are formed by filamentous fungi and play a role in fungal growth. Furthermore, hydrophobins make fungal spores hydrophobic (Linder et al., 2005). On the contrary, mannitol acts as hygroscopic sugars and actively participates in dispersing spores via coalescing droplets formed on the mushrooms (Hassett et al., 2015). Thus, we employ octanol–water distribution coefficients to identify the degree of hydrophobicity of fungal particles collected from the atmosphere. Traditionally, octanol–water distribution

coefficient has been widely used in many areas such as drug design and pharmaceuticals, substance toxicology, and modelling of environmental fate of organic chemicals (Sangster, 1988). The octanol–water distribution coefficient of a compound is derived by calculating the ratio of the compound distributed between two immiscible phases, octanol and water. The octanol–water distribution coefficient is a unitless value because it is the ratio of concentrations in the two phases. The octanol–water distribution coefficient of one compound can be different from that of other compounds because the polarity of each compound is different. Therefore, the octanol–water distribution coefficients can be used to compare the degree of hydrophobicity of various compounds. Here, the octanol–water distribution coefficient was utilized to estimate hydrophobicity and hydrophilicity of fungal particles collected from the atmosphere in Seoul, South Korea. We adopted the frozen water phase method (Yamashita et al., 2011) because it prevents contamination of octanol on the frozen water phase and is a more suitable technique for separating particles in the octanol–water phase system as opposed to other octanol–water partitioning methods. For example, one of the conventional octanol–water partition method, the shake-flask method, is a simple and widely used method, but it was not appropriate for our experimental purpose, i.e., separation of particles.

In this study, airborne fungal particles were collected from the atmosphere using a two-stage cyclone sampler (Lindsley et al., 2006) between June 14 and November 08 in 2016. The collected fungal particles were divided based on their surface properties using the frozen water phase method. The taxon-specific octanol–water distribution coefficients of the fungal particles were determined by quantifying each taxon in each phase by employing a combination of quantitative PCR (qPCR) and high-throughput

sequencing methods (An et al., 2017). Cluster analysis was conducted to reveal whether the octanol–water distribution coefficients in the genus rank are phylogenetically related or not. Furthermore, the correlation analysis and the generalized linear model were utilized to identify whether the octanol–water distribution coefficients of the fungal particles are affected by the environmental factors, climatological conditions, and concentration of anthropogenic air pollutants per week. Therefore, this research is expected to play an important role in confirming the degree of hydrophobicity of taxon-specific fungal particles from the kingdom to the genus level and their potential association with the environmental factors.

2. Materials and Methods

2.1. Air sampling

Weekly air samplings were conducted consecutively from June 14 to November 08 in 2016 using two two-stage cyclone samplers (Lindsley et al., 2006) at the rooftop of the building of the Graduate School of Public Health at Seoul National University in South Korea (37º27′55.0″N, 126º57′17.7″E, ~20 m above the ground). The samplings were performed in duplicates from July 19 to November 8 in 2016. Each of the collocated duplicated two-stage cyclone samplers was operated using the MP-Σ300 and MP-Σ300NII mini pumps (Sibata Scientific Technology, Ltd., Tokyo, Japan), with the flow rate adjusted to 2 $L \cdot min^{-1}$. The cut-off aerodynamic diameters (d_a) of the first and second stages of the cyclone sampler are 2.6 and 1.6 μm, respectively (Lindsley et al., 2006). A 1.5-mL microcentrifuge tube with a conical screw cap (#SCT-150-C-S, Axygen Scientific, Inc. USA) was attached to each stage of the sampler. The samples collected in the tubes of the first stage (d_a>2.6 μm) were used for subsequent sequencing and qPCR analyses because most of the airborne fungal particles were collected at the first stage (Lindsley et al., 2006 and Yamamoto et al., 2012). Seventy-two sampled tubes of the first stage of the cyclone samplers were kept at −20ºC until subsequent analyses.

2.2. Separation of airborne fungal particles into the octanol and water phases

The method reported by Yamashita et al. (2011) was used to separate the collected airborne fungal spores into the octanol and water phases. Twenty milliliter of 1-

octanol (CAS 111-87-5, Sigma Aldrich, Seoul, South Korea) and 20 mL of ultrapure water (Product No. W2006; Autoclaved; no DNase detected; Biosesang, Seongnam, South Korea) were mixed and mutually pre-saturated in a 50-mL conical tube for 24 h by gently shaking at 25ºC. After shaking, the tube was placed without any agitation for 24 h at 25ºC, after which the mutually pre-saturated octanol and water phases were divided into two 50-mL conical tubes. Four hundred and fifty microliter of pre-saturated 1-octanol and 900 μL of pre-saturated ultrapure water were added to each of the sampled 1.5-mL tubes. The tubes were gently shaken overnight at 25ºC. After shaking, the tubes were placed vertically for 1 h to separate octanol and water phases completely. The tubes were then exposed to liquid nitrogen for approximately1 min to freeze only the water phase. The unfrozen 1-octanol was recovered from the tubes and added to 30 mL of 50% ethanol solution. The remnant 1-octanol on the frozen water was recovered by washing and recovering with 600 μL of fresh 1-octanol followed by washing and recovering with 600 μL of 50% fresh ethanol. After the washing-out step, the thawed water phase was recovered and added into another 30 mL of 50% ethanol solution. Airborne fungal spores partitioned into the octanol and water phases, which were separately recovered into 30 mL of 50% ethanol, were filtrated using the MiroFunnel™ Filter Funnel (#PN4800; 0.45 μm GN-6 Mericel® membrane; white, gridded, and sterile; Pall Life Sciences, USA). One-quarter fraction of each filter was used for DNA extraction.

2.3. DNA extraction and quantitative PCR

The DNA extraction method reported by Hospodsky et al. (2010) was used. Briefly, the fungal DNA in the one-quarter fraction of each filter was used for subsequent

analysis using qPCR and DNA sequencing. The PowerMax® Soil DNA Isolation Kit (Mobio Laboratory, Carlsbad, CA, USA) was utilized for DNA extraction after some modifications. Glass beads measuring 0.1 mm (300 mg) and 0.5 mm in diameters (100 mg) were added to 2-mL kit's tubes containing kit's power beads (1.0 g). One-quarter fraction of each filter was cut using sterile scissors. The samples in the tubes were homogenized for 3 min using a bead beater (BioSpec Products, Bartlesville, OK, USA), and DNA from each sample was extracted using the method described by the manufacturer. DNA was eluted into 50 µl of TE (10 mM Tris-HCl, 1 mM EDTA, pH=8.0).

qPCR was conducted to measure gene copy number (GCN) of the fungal internal transcribed spacer 1 (ITS1) region (Schoch et al., 2012) in the separated octanol and water phases and consequently calculate octanol–water distribution coefficients of each sample. The quantitative PCR method reported by Kumari et al. (2016) was employed after making some modifications. Briefly, the ITS1 region was amplified using the universal fungal primers of ITS1F (5′-CTTGGTCATTTAGAGGAAGTAA-3′) and ITS2 (5′-GCTGCGTTCTTCATCGATGC-3′) (Gardes and Bruns, 1993; White et al., 1990). Each of the 20 µL reaction mixtures contained 15 µL of 2× concentrated LightCycler® 480 SYBR Green I Master (Cat. No. 04-707-516-001, Roche Diagnostics Ltd., Lewes, UK), 0.4 µL each of 10 µM forward and reverse primers, 8.2 µl of PCR-grade water, and 1 µl of DNA from each sample. The LightCycler® 480 Real-Time PCR System (Roche Applied Science, Indianapolis, IN, USA) was used for qPCR analysis. The thermal cycle profile of qPCR was as follows: 15-min initial denaturation at 95ºC; 45 cycles of 15-s dissociation at 95ºC; and 1-min annealing and extension at 60ºC.

Standard curves were created by ITS1 amplicon of *Aspergillus fumigatus* (ATCC MYA 4609) with the same universal primers. Quant-iT PicoGreen dsDNA reagent kit (Life Technologies, Carlsbad, CA, USA) quantified the concentration of the standard 1 to 10^6 GCN μL^{-1} to 1 to 10^0 GCN μL^{-1} for calibrating qPCR. Every measurement for each sample was performed in triplicates, and PCR inhibition was examined using the method described by Hospodsky et al. (2010). PCR inhibitions were not detected in all samples. A DNA extraction efficiency value of 10% was assumed to calculate GCN per individual volumes of separated octanol or water phases for each sample (Hospodsky et al., 2010).

2.4. High-throughput DNA sequencing and analysis

High-throughput DNA sequencing was performed for elucidating community diversities of airborne fungi in the atmosphere and for calculating octanol–water distribution coefficients of each sample. The method reported by An et al. (2016) was used for high-throughput DNA sequencing and subsequent analysis. Briefly, the ITS1 region of each sample was targeted by ITS1F and ITS2 primers with adapter sequences for the Illumina Miseq. Each PCR reaction volume was 30 µL, including 15 µL of 2× concentrated PCR Solution Premix Taq™ DNA polymerase (Takara Bio Inc., Otsu, Shiga, Japan), 1 µL each of 10 µM ITS1F and ITS2F primers, 12 µL of PCR-grade water, and 1 µL of template from each sample. The thermal cycle of PCR was as follows: 5-min incubation at 95ºC followed by 35 cycles of 30 s at 95ºC, 30 s at 55ºC, and 30 s at 72ºC. Final elongation was at 72ºC for 10 min by T100™ thermal cycler (Bio-Rad Laboratories, Inc., Hercules, CA, USA). After PCR, the AMPure XP beads (Beckman Coulter, Inc., Brea, CA, USA) were used for purifying PCR products. Using the Nextera

XT Index kit (Illumina, Inc., San Diego, CA, USA), the purified PCR products were subjected to Index PCR. Fifty microliter of the Index PCR reaction mixture comprised 25 μL of 2× concentrated PCR Solution Premix Taq™ DNA polymerase (Takara Bio Inc.), 5 μL of each index primer, 15 μL of PCR-grade water, and 5 μL of the purified DNA from each sample. The thermal conditions of Index PCR were 3-min incubation at 95ºC, 10 cycles of 30 s at 95ºC, 30 s at 55ºC, and 30 s at 72ºC. Final elongation was at 72ºC for 5 min. Following the Index PCR step, the amplicons of Index PCR were purified by AMPure XP beads (Beckman Coulter, Inc.) and then normalized to 4 nM with 10 mM Tris-HCl (pH=8.5). After the normalization step, each amplicon was pooled with an internal control PhiX (30%). Pooled amplicons were denatured by heat and loaded to a v3 600 cycle-kit reagent cartridge (Illumina, Inc.), and 2 × 300 base pair paired-end sequencing was performed using the Illumina MiSeq at the Graduate School of Public Health, Seoul National University. Raw sequence data is accessible in the Sequence Read Archive of the National Center for Biotechnology Information (NCBI) under the project number SRP127209.

The raw sequences were refined using several bioinformatics tools. MiSeq Reporter v2.5 (Illumina, Inc.) demultiplexed and trimmed the raw sequences with a read quality score above 20. After modifying the raw sequences, Trimmomatic-0.36 (Bolger et al., 2014) trimmed the poly-N tail sequences of all the sequences. In the absence of poly-N tail sequences of each sequence, the Quantitative Insights Into Microbial Ecology (QIIME) (Caporaso et al., 2010) software was used for joining read 1 and read 2 sequences with a minimum allowed overlap of 10 base pair. Mothur v.1.35.1 (Schloss et al., 2009) was used for removing chimeric sequences of the joined sequences by

searching a reference database, i.e., fungal ITS sequences (Nilsson et al., 2009). Following the removal of the chimeric sequences, Galaxy Tool Version 17.05 (Afgan et al., 2016) filtered the sequences with a minimum threshold length of 100 base pair. The sequences after the consecutive processes were taxonomically assigned by BLASTN2.2.28+ (Altschul et al., 1990) against the fungal ITS sequences (Nilsson et al., 2009) and classified using the FHiTHINGS bioinformatics tool (Dannemiller et al., 2014b).

2.5. Octanol–water distribution coefficient

Octanol–water distribution coefficient ($D_{oct/wat}$) was defined as the ratio of absolute concentration of a fungal taxon in the octanol phase divided by the absolute concentration of that taxon in the water phase. First, the octanol–water distribution coefficients at the kingdom level were obtained using the qPCR-derived fungal GCN ratio of the separated octanol and water phases based on the 36 pairs of samples collected weekly. Furthermore, the taxon-specific octanol–water distribution coefficients at the phylum and genus levels were derived based on 28 pairs of samples. Among 36 pairs of samples obtained in a week, 12 samples were excluded because of low-quality sequencing data and 4 samples were excluded because they lost one of the pairs (Supplementary Table 3). The taxon-specific absolute concentration of each phase was calculated using the qPCR-derived fungal GCN multiplied by the relative abundance of each taxon from the sequencing data. Since relative abundances at lower taxonomic ranks, such as family and genus ranks, showed 0% for many samples, we added one to the natural logarithm of all taxon-specific absolute concentrations. Then, the taxon-

specific octanol–water distribution coefficients calculated by the base 10 logarithm of the modified concentrations in the octanol phase divided by the modified concentrations in the water phase (1.1).

$$\log_{10} D_{\mathrm{oct/wat}} = \log_{10}\left(\frac{\mathrm{EXP}[\ln(Absolute\ \ concentration_{Octanol})+1]}{\mathrm{EXP}[\ln(Absolute\ \ concentration_{Water})+1]} \right) \quad (1.1)$$

2.6. Statistical analysis

The Statistical Analysis System (SAS) 9.4 (SAS Institute Inc., Cary, NC, USA) software was utilized for statistical analysis. Paired *t*-test was performed using the octanol–water distribution coefficients of the fungal kingdom to check statistically meaningful differences among each of the observations across the total period of sampling, which was performed in duplicates. In addition, the paired *t*-test was utilized to identify the statistically meaningful differences between the phylum-specific octanol–water distribution coefficients of Ascomycota and Basidiomycota across the sampling periods.

The hierarchical cluster analysis was used for identifying whether genetically similar fungi at genus rank tended to have similar surface properties, such as degree of hydrophobicity. For the hierarchical cluster analysis, we obtained the distance matrix using the DCORR option of SAS. Moreover, we used Ward's minimum variance method for this analysis.

The one-way mixed-effect model was used to compare the variance of the octanol–water distribution coefficients at the kingdom level between and within sampling periods. Furthermore, the Spearman's correlation analysis was employed to

reveal a potential relationship among the octanol–water distribution coefficients at the kingdom level as well as the taxonomic effects, climatological conditions, and weekly concentration of anthropogenic air pollutants. The taxon-specific relative abundance of fungal class across each sampling period was considered as the taxonomic effects. The fungal class-specific relative abundance across each sampling period was calculated as the sum of absolute concentrations specific to each class in the octanol and water phases divided by the sum of fungal kingdom concentration in the two phases (2.1).

$$Class\ specific\ relative\ abundance = \frac{AC\ in\ octanol_{Fungal\ class} + AC\ in\ water_{Fungal\ class}}{Concentration\ in\ octanol_{Fungal\ kingdom} + Concentration\ in\ water_{Fungal\ kingdom}} \quad (2.1)$$

For assessing climatological conditions, the temperature, relative humidity, wind speed, and total amount of weekly precipitation were considered. The data were obtained from the South Korea Meteorological Administration (Supplementary Table 1). Furthermore, the weekly concentrations of anthropogenic air pollutants in the atmosphere of Seoul, South Korea, were obtained from the Ministry of Environment of South Korea (Supplementary Table 2).

The generalized linear model was utilized for exploring meaningful parameters that can affect the variations in octanol–water distribution coefficients at the kingdom level. Thus, we considered the duplicate as a repeated measurement and each sampling period as a random effect. The parameters included taxonomic effects, climatological conditions, and weekly concentration of anthropogenic air pollutants. We used stepwise backward elimination for the parameter selection at a significance level of 0.10.

3. Results

3.1. Fungal taxon-specific octanol–water distribution coefficients

Octanol–water distribution coefficients of fungal particles were obtained at the fungal kingdom, phylum, class, order, family, and genus levels. The octanol–water distribution coefficients of fungal particles at the kingdom level across the sampling periods are summarized in Table 1 and shown in Figure 1. The paired *t*-test implied that the octanol–water distribution coefficients of the duplicate experiments were not significantly different ($p>0.05$). Among 36 observations across total sampling periods, the number of hydrophobic observations ($\log_{10}D_{oct/wat}>0$) was 27 and the number of hydrophilic observations ($\log_{10}D_{oct/wat}<0$) was 9. The observations in the sampling period 6, 7, and 18 showed higher hydrophobicity than other sampling periods.

The majority of fungal particles belonged to the phyla Ascomycota and Basidiomycota and the mean relative abundance of Ascomycota and Basidiomycota phyla were 64.2% and 35.6%, respectively. The octanol–water distribution coefficients of fungal particles in the phylum rank across total sampling period are summarized in Table 2. The paired *t*-test implied that the octanol–water distribution coefficients of the two major phyla were not significantly different ($p>0.05$). The octanol–water distribution coefficients of Ascomycota and Basidiomycota phyla showed similar patterns of variation caused by different sampling periods (Figure 2). For lower taxonomic-level analyses, we established a criterion that the number of octanol–water distribution coefficients of each taxon should have at least 10 individual octanol–water distribution coefficients among 17 sampling periods, while duplicates were considered as an individual octanol–water distribution coefficient. Furthermore, class, order, and family

ranks, which do not contain a genus that meets the aforementioned criterion, were excluded. Consequently, 9 classes, 19 orders, 35 families, and 63 genera were selected for subsequent analysis. The octanol–water distribution coefficients of fungal particles at the class, order, family, and genus levels are summarized in Tables 3–6, respectively.

Table 1. The octanol–water distribution coefficients of fungal particles at the kingdom level across the sampling periods.

Sample ID	Sampling period ID	Sampling start day (yymmdd)	Sampling end day (yymmdd)	Duplicate	Concentration in octanol (GCN[1]/mL)	Concentration in water (GCN[1]/mL)	$\log_{10}D_{oct/wat}$ of fungi
OW1D1	1	160614	160621	1	1491883	387274	0.59
OW2D1	2	160621	160628	1	5887947	3817104	0.19
OW4D1	4	160705	160712	1	381928	813401	–0.33
OW5D1	5	160712	160719	1	768188	2147644	–0.45
OW6D1	6	160719	160726	1	814056	31028	1.42
OW6D2				2	456795	40948	1.05
OW7D1	7	160726	160802	1	2211695	69835	1.50
OW7D2				2	2276453	76623	1.47
OW8D1	8	160802	160809	1	772692	1251439	–0.21
OW8D2				2	827363	307434	0.43
OW9D1	9	160809	160816	1	631153	209676	0.48
OW9D2				2	62055	93339	–0.18
OW10D1	10	160816	160823	1	1565625	819511	0.28
OW10D2				2	1753976	1115335	0.20
OW11D1	11	160823	160830	1	9523561	1434951	0.82
OW11D2				2	6331953	994634	0.80
OW12D1	12	160831	160907	1	98343	406231	–0.62
OW12D2				2	1317113	680869	0.29
OW13D1	13	160907	160914	1	1209324	587288	0.31
OW13D2				2	526852	95348	0.74
OW14D1	14	160914	160921	1	992462	3571182	–0.56
OW14D2				2	6556392	220392	1.47

OW15D1	15	160921	160928	1	2959307	2053625	0.16
OW15D2				2	2488451	730594	0.53
OW16D1	16	160928	161005	1	6158319	1455144	0.63
OW16D2				2	8266374	1861673	0.65
OW17D1	17	161005	161012	1	2551586	805923	0.50
OW17D2				2	8529359	3354357	0.41
OW18D1	18	161012	161019	1	4251528	320263	1.12
OW18D2				2	2385648	596786	0.60
OW19D1	19	161020	161027	1	11937502	10216294	0.07
OW19D2				2	6126703	11122339	–0.26
OW20D1	20	161027	161103	1	6798807	12186152	–0.25
OW20D2				2	7723015	10842397	–0.15
OW21D1	21	161103	161108	1	2301032	1416786	0.21
OW21D2				2	3394320	693939	0.69
Mean							0.41
Standard deviation							0.58

[1]Gene copy number

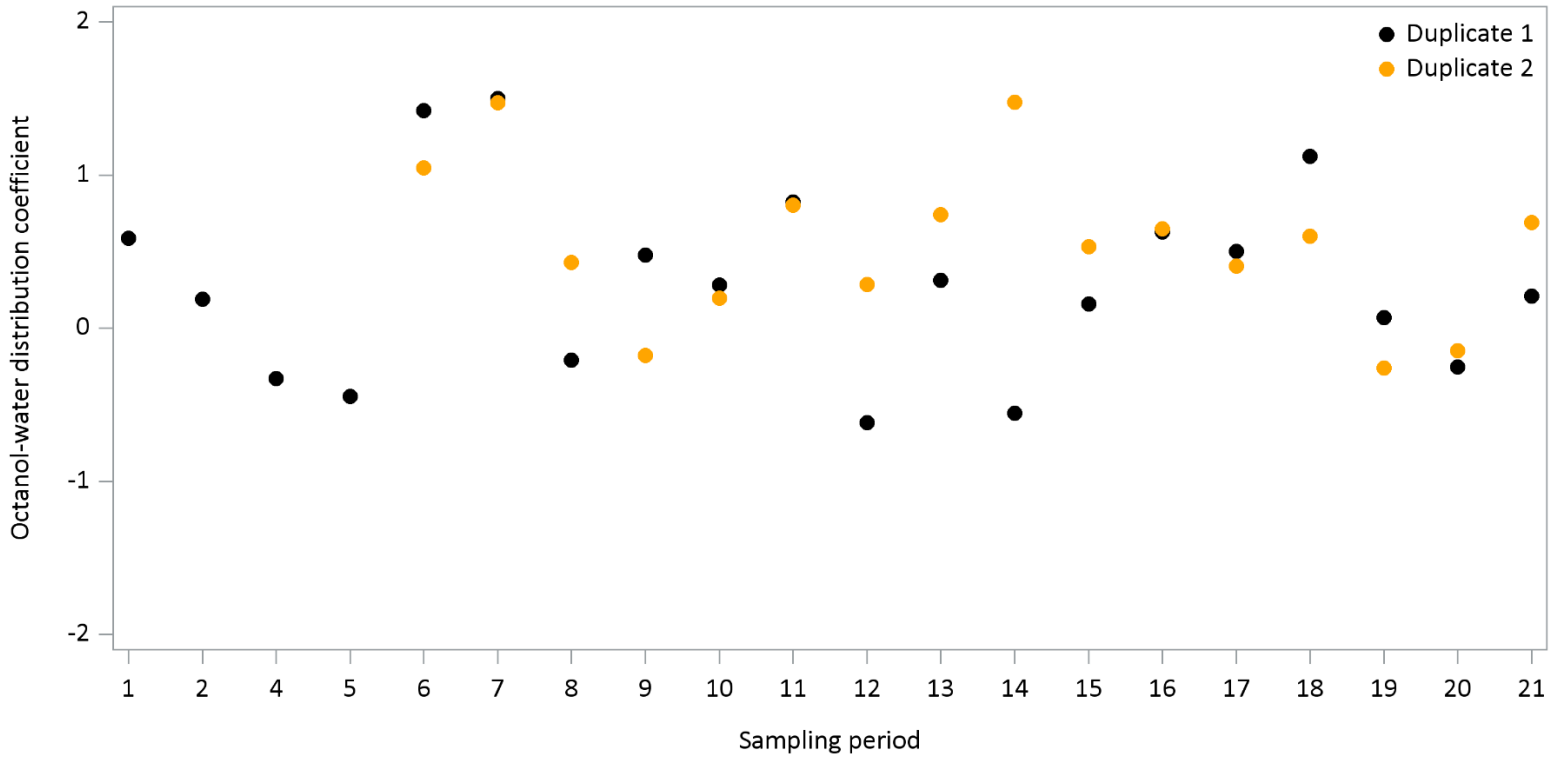

Figure 1. The octanol–water distribution coefficients at the kingdom level across the sampling periods. The paired *t*-test implied that the octanol–water distribution coefficients of duplicates were not significantly different ($p>0.05$).

Table 2. The octanol–water distribution coefficients of fungal particles at the phylum level across the sampling periods.

Sample ID	Absolute Concentration[1] in octanol		Absolute concentration[1] in water		$\log_{10}D_{oct/wat}$ of	$\log_{10}D_{oct/wat}$ of
	Ascomycota	Basidiomycota	Ascomycota	Basidiomycota	Ascomycota	Basidiomycota
OW1D1	1481773	10110	338464	48488	0.64	–0.68
OW2D1	5842931	44837	3810145	6959	0.19	0.81
OW4D1	156237	225691	609690	203711	–0.59	0.04
OW5D1	401716	366391	1610336	529662	–0.60	–0.16
OW7D1	1214974	996721	34115	35720	1.55	1.45
OW7D2	962577	1302521	25766	50857	1.57	1.41
OW8D2	254615	572347	269685	37749	–0.02	1.18
OW10D1	902475	663150	341572	477939	0.42	0.14
OW11D1	6800338	2697010	828635	606316	0.91	0.65
OW11D2	4407209	1924565	651005	342241	0.83	0.75
OW12D1	36141	62200	260989	145242	–0.86	–0.37
OW12D2	1120158	193328	474703	205955	0.37	–0.03
OW13D1	1102601	86308	475458	111488	0.37	–0.11
OW13D2	494083	32769	57908	37439	0.93	–0.06
OW15D1	825116	2133399	402499	1650968	0.31	0.11
OW15D2	662835	1808956	243210	487273	0.44	0.57
OW16D1	4130552	2000269	593195	841829	0.84	0.38
OW16D2	4957002	3213923	1094352	765071	0.66	0.62
OW17D1	2157444	394116	603877	191525	0.55	0.31
OW17D2	7658754	870517	2736951	595851	0.45	0.16
OW18D1	2453175	1798353	271305	48958	0.96	1.57
OW18D2	1644884	740637	450982	145804	0.56	0.71
OW19D1	7266306	4671196	3576913	6620234	0.31	–0.15

OW19D2	2229357	3884184	3644862	7458495	–0.21	–0.28
OW20D1	5426669	1370188	8342393	3797959	–0.19	–0.44
OW20D2	7405822	315097	7722775	3108857	–0.02	–0.99
OW21D1	1279157	1017524	1033663	371234	0.09	0.44
OW21D2	2992803	401517	489980	197027	0.79	0.31
Mean					0.40	0.30
Standard deviation					0.58	0.63

[1]Relative abundance × Concentration in octanol or water (GCN/mL)

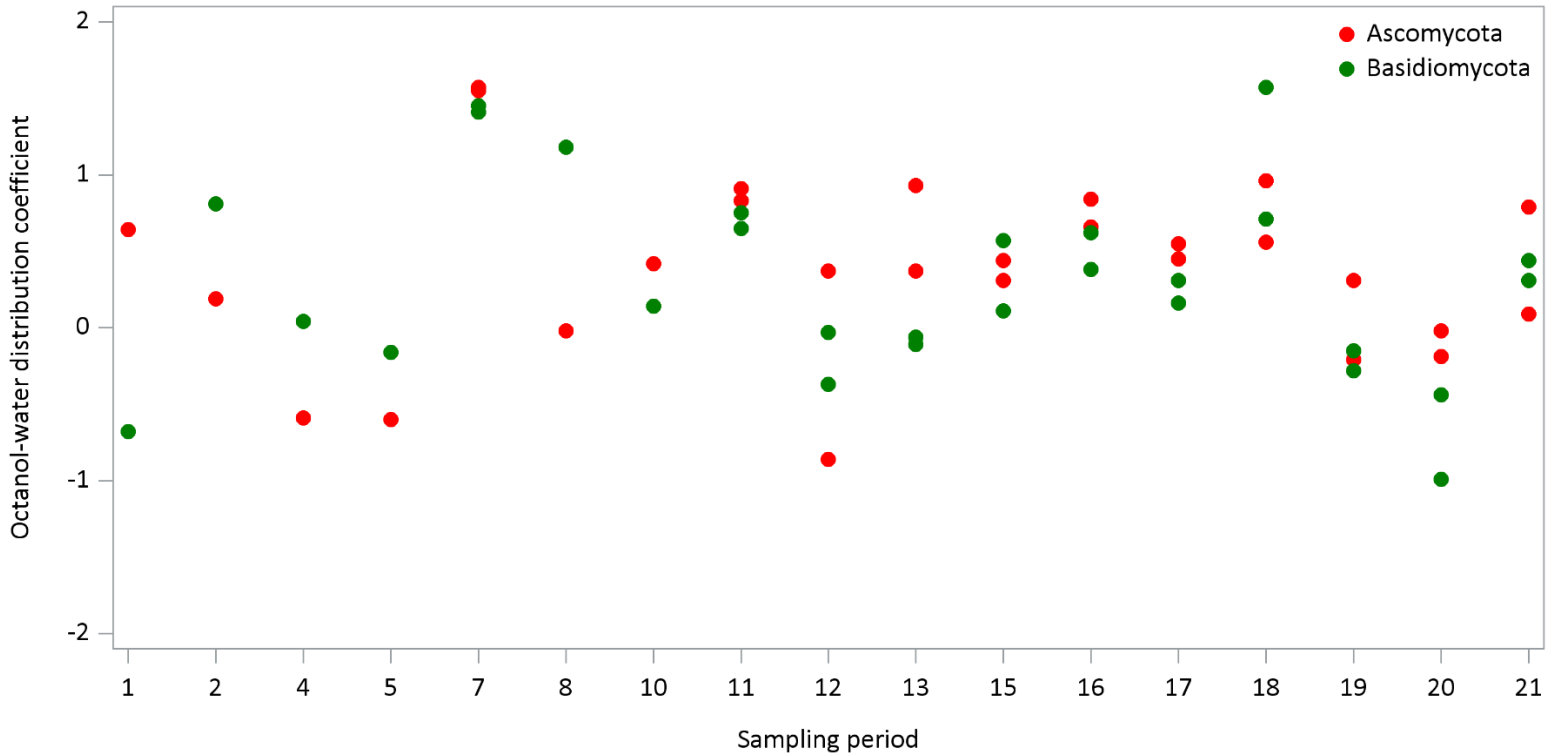

Figure 2. The octanol–water distribution coefficients of Ascomycota and Basidiomycota across the sampling periods. The octanol–water distribution coefficients of Ascomycota and Basidiomycota showed similar patterns of variation affected by the sampling period.

Table 3. The octanol–water distribution coefficients of fungal particles at the class level. Taxonomic classification was referenced against the Index Fungorum.

Phylum	Class	Mean relative abundance (%)	N	Mean of $\log_{10}D_{oct/wat}$	Standard deviation of $\log_{10}D_{oct/wat}$
Ascomycota	Dothideomycetes	35	28	0.64	0.97
	Sordariomycetes	21	28	0.18	1.08
	Leotiomycetes	3.3	28	0.57	2.01
	Eurotiomycetes	1.2	25	0.51	2.45
Basidiomycota	Agaricomycetes	32	28	0.28	0.69
	Tremellomycetes	1.4	21	0.40	2.34
	Dacrymycetes	1.1	20	–0.28	3.06
	Microbotryomycetes	0.6	16	0.91	2.87
	Malasseziomycetes	0.02	14	0.79	2.35

Table 4. The octanol–water distribution coefficients of fungal particles at the order level. Taxonomic classification was referenced against the Index Fungorum.

Class	Order	Mean relative abundance (%)	N	Mean of $\log_{10}D_{oct/wat}$	Standard deviation of $\log_{10}D_{oct/wat}$
Dothideomycetes	Capnodiales	22	28	1.06	1.43
	Dothideales	0.4	24	–0.95	1.86
	Pleosporales	12	28	0.31	1.20
Sordariomycetes	Sordariales	8.7	28	–0.82	2.09
	Xylariales	2.8	26	–0.27	1.93
	Hypocreales	2.3	27	0.40	1.68
Leotiomycetes	Helotiales	2.1	26	0.87	2.01
	Erysiphales	1.1	25	0.74	3.28
Eurotiomycetes	Eurotiales	0.8	22	1.31	2.37
Agaricomycetes	Agaricales	10	28	0.42	1.34
	Geastrales	0.1	15	0.93	2.84
	Polyporales	15	28	0.38	1.29
	Russulales	3.0	26	–0.21	2.22
	Hymenochaetales	1.4	26	–0.39	2.51
	Trechisporales	0.6	18	0.60	2.90
Tremellomycetes	Tremellales	1.3	21	0.38	2.32
Dacrymycetes	Dacrymycetales	1.1	20	–0.28	3.06
Microbotryomycetes	Sporidiobolales	0.6	16	0.60	3.26
Malasseziomycetes	Malasseziales	0.02	14	0.79	2.35

Table 5. The octanol–water distribution coefficients of fungal particles at the family level. Taxonomic classification was referenced against the Index Fungorum.

Order	Family	Mean relative abundance (%)	N	Mean of $\log_{10}D_{oct/wat}$	Standard deviation of $\log_{10}D_{oct/wat}$
Capnodiales	Cladosporiaceae	0.6	28	0.92	1.40
	Teratosphaeriaceae	0.4	24	–0.93	2.74
	Davidiellaceae	0.1	16	0.88	2.90
Dothideales	Saccotheciaceae	0.3	22	–1.20	1.62
Pleosporales	Pleosporaceae	9.6	28	0.17	1.66
	Didymellaceae	1.2	22	–0.19	3.83
	Lophiostomataceae	0.4	17	–0.90	3.24
	Coniothyriaceae	0.2	17	–0.77	3.66
Sordariales	Sordariaceae	6.1	17	0.65	2.38
	Lasiosphaeriaceae	2.2	28	–1.63	1.97
	Chaetomiaceae	0.4	19	–1.22	3.04
Xylariales	Diatrypaceae	2.2	22	–0.97	2.52
Hypocreales	Nectriaceae	1.0	26	–0.18	2.74
	Ophiocordycipitaceae	0.1	19	0.42	2.17
Helotiales	Sclerotiniaceae	1.4	26	1.23	2.15
Erysiphales	Erysiphaceae	1.1	25	0.74	3.28
Eurotiales	Trichocomaceae	0.7	22	1.32	2.37
Agaricales	Agaricaceae	3.3	25	1.29	2.34
	Physalacriaceae	1.7	24	–0.31	2.42
	Psathyrellaceae	1.3	17	0.07	2.83
	Cortinariaceae	0.3	15	0.72	2.66
Geastrales	Geastraceae	0.1	15	0.93	2.84
Polyporales	Polyporaceae	4.6	27	–0.23	2.04
	Meruliaceae	4.1	27	0.45	2.32
	Fomitopsidaceae	2.7	27	–0.02	2.23
	Ganodermataceae	1.8	22	0.52	3.15
	Phanerochaetaceae	1.4	23	0.92	2.73
Russulales	Peniophoraceae	1.3	20	–0.16	2.76
	Bondarzewiaceae	0.6	16	–0.04	3.01
Hymenochaetales	Hymenochaetaceae	0.4	19	0.16	3.22
	Schizoporaceae	0.4	22	–0.77	2.82
Trechisporales	Hydnodontaceae	0.6	18	0.60	2.90
Tremellales	Tremellaceae	1.0	20	–0.01	2.77
Dacrymycetales	Dacrymycetaceae	1.1	20	–0.28	3.06
Malasseziales	Malasseziaceae	0.02	14	0.79	2.35

Table 6. The octanol–water distribution coefficients of fungal particles at the genus level. Taxonomic classification was referenced against the Index Fungorum.

Family	Genus	Mean relative abundance (%)	N	Mean of $\log_{10}D_{oct/wat}$	Standard deviation of $\log_{10}D_{oct/wat}$
Cladosporiaceae	*Cladosporium*	0.6	28	0.92	1.40
Teratosphaeriaceae	*Catenulostroma*	0.2	14	–0.83	2.68
	Teratosphaeria	0.1	18	–0.89	2.58
Davidiellaceae	*Davidiella*	0.1	16	0.88	2.90
Saccotheciaceae	*Aureobasidium*	0.3	22	–1.19	1.62
Pleosporaceae	*Alternaria*	5.1	28	0.51	2.37
	Cochliobolus	0.1	12	–1.39	2.94
Didymellaceae	*Epicoccum*	3.8	25	–0.19	2.48
	Leptosphaerulina	1.2	19	0.03	3.70
	Phoma	0.2	14	–1.67	2.33
	Stagonosporopsis	0.1	14	–1.37	2.84
Lophiostomataceae	*Lophiostoma*	0.4	17	–0.90	3.24
Coniothyriaceae	*Coniothyrium*	0.2	17	–0.77	3.66
Sordariaceae	*Sordaria*	6.1	17	0.65	2.38
Lasiosphaeriaceae	*Fimetariella*	2.0	28	–1.62	1.95
	Cercophora	0.1	25	–1.28	1.54
Chaetomiaceae	*Chaetomium*	0.4	18	–1.22	3.10
Incertae cedis	*Rhodoveronaea*	0.4	19	0.30	3.36
Diatrypaceae	*Eutypella*	2.1	19	–0.51	2.26
Nectriaceae	*Neonectria*	0.5	15	–1.64	3.45
	Fusarium	0.4	17	–0.14	2.86
	Nectria	0.04	20	–0.48	2.04
Ophiocordycipitaceae	*Hirsutella*	0.02	13	0.27	2.46
Incertae cedis	*Myrothecium*	0.1	16	0.01	3.19
	Acremonium	0.1	20	0.31	2.77
Incertae cedis	*Nigrospora*	5.4	26	–0.42	3.02
Sclerotiniaceae	*Botryotinia*	0.4	16	–0.15	2.81
Incertae cedis	*Trimmatostroma*	0.5	15	–1.25	3.13
Erysiphaceae	*Sawadaea*	0.3	13	1.99	3.07
	Podosphaera	0.2	15	0.30	3.49
Trichocomaceae	*Penicillium*	0.5	23	1.23	2.73
	Eurotium	0.4	15	2.15	2.15
	Aspergillus	0.3	21	1.22	2.51
Incertae cedis	*Noosia*	2.0	24	1.45	1.85
	Knufia	0.2	16	–0.78	2.79

Agaricaceae	*Handkea*	1.7	17	1.60	2.52
	Lycoperdon	0.5	17	1.64	2.37
Physalacriaceae	*Flammulina*	1.1	12	–1.24	3.37
Psathyrellaceae	*Psathyrella*	1.0	15	–0.14	2.54
	Coprinopsis	0.5	19	–0.63	2.93
Cortinariaceae	*Cortinarius*	0.3	15	1.16	2.96
Geastraceae	*Geastrum*	0.1	15	0.93	2.84
Polyporaceae	*Perenniporia*	1.7	26	–1.30	2.32
	Trametes	1.5	21	0.34	2.85
	Polyporus	0.1	16	0.78	2.99
Meruliaceae	*Irpex*	2.2	20	0.77	2.10
	Phlebia	0.7	20	0.31	2.64
	Hyphoderma	0.5	15	0.27	3.94
	Bjerkandera	0.2	13	–1.10	3.44
Fomitopsidaceae	*Fomitella*	2.4	26	–0.75	2.32
Ganodermataceae	*Ganoderma*	1.8	22	0.52	3.15
Phanerochaetaceae	*Phanerochaete*	0.5	16	0.85	3.45
	Antrodiella	0.4	17	1.25	3.19
Peniophoraceae	*Peniophora*	1.3	20	–0.16	2.76
Bondarzewiaceae	*Heterobasidion*	0.6	16	–0.04	3.01
Hymenochaetaceae	*Fuscoporia*	0.2	15	0.59	4.12
Schizoporaceae	*Hyphodontia*	0.4	19	–1.25	3.06
Incertae cedis	*Trichaptum*	0.5	20	–0.87	2.44
Hydnodontaceae	*Trechispora*	0.6	18	0.46	2.95
Tremellaceae	*Cryptococcus*	0.7	17	–1.02	2.34
Dacrymycetaceae	*Cerinomyces*	0.8	18	–0.80	2.75
Incertae cedis	*Sporobolomyces*	0.3	14	0.43	3.16
Malasseziaceae	*Malassezia*	0.02	14	0.79	2.35

3.2. Hierarchical cluster analysis

The hierarchical cluster analysis was conducted to reveal whether the octanol–water distribution coefficient at the genus level has a phylogenetic relationship. The result of hierarchical cluster analysis showed that fungal genera were not taxonomically clustered by the octanol–water distribution coefficients (Figure 3). Few genera that belonged to the same order rank such as *Cercophora* and *Fimetariella*, *Podosphaera* and *Sawadaea,* and *Stagonosporopsis* and *Cochliobolus* showed higher similarity with regard to the octanol–water distribution coefficients in the genus rank across the sampling period compared with other genera. However, in most cases, as the clustering progresses, the genera belonging to the same phylum rank but to a different order rank or the genera belonging to a different phylum were clustered together in the same cluster with relatively higher similarity (R^2>0.7). Overall, the octanol–water distribution coefficients of fungal particles, in other words, the degree of hydrophobicity of fungal particle surface showed high intra-variation for the two phyla.

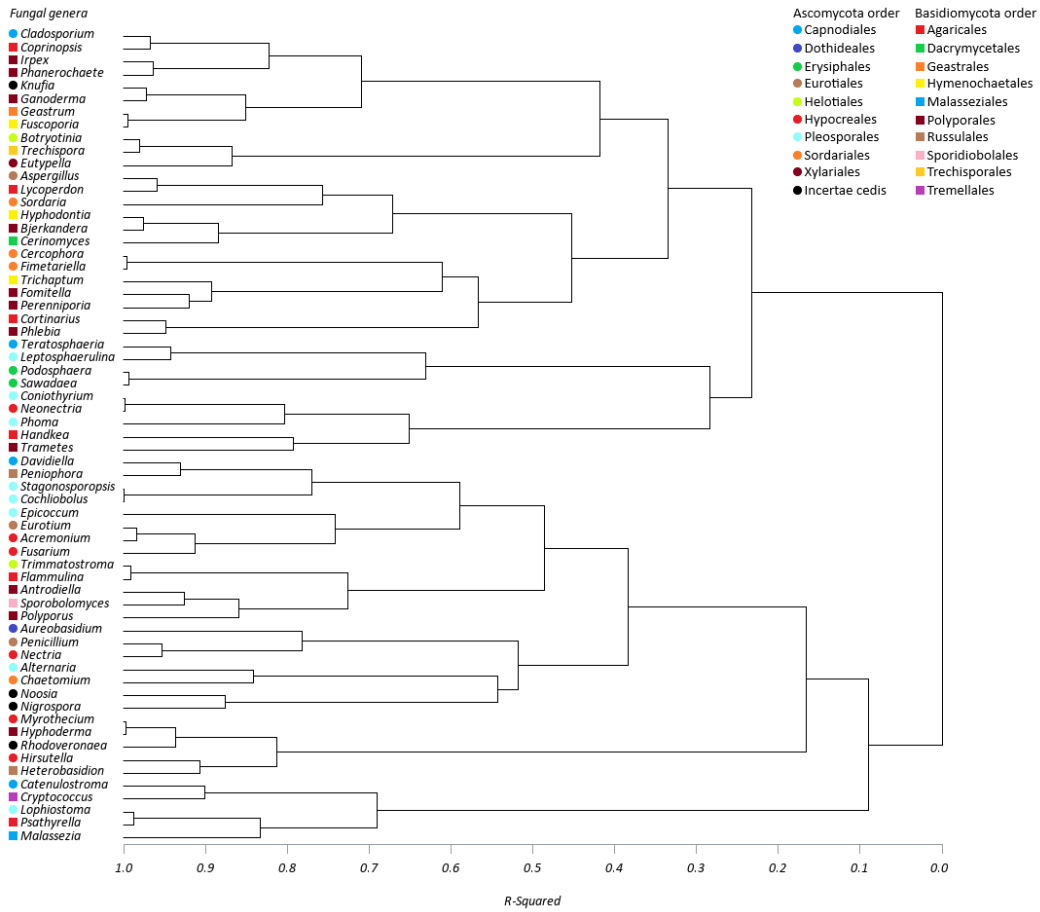

Figure 3. Hierarchical cluster analysis based on the octanol–water distribution coefficients at the genus level. Fungal genera were not taxonomically clustered by the octanol–water distribution coefficients. Fungal particles of each genus were presented at the order level, and the taxonomy of each genus was referenced against the Index Fungorum. Ascomycota and Basidiomycota orders are shown as colored circle and rectangle, respectively. A tree was constructed based on the DCORR option of SAS used for determining the distance matrix and on Ward's minimum variance cluster method.

3.3. Variability of octanol–water distribution coefficients across the sampling periods

The fungal taxon-specific octanol–water distribution coefficients widely varied depending on the sampling periods and species (Tables 1–6). To generalize and explain the variability of the octanol–water distribution coefficients, these coefficients at the fungal kingdom level were used for subsequent analysis. Because the result of the paired *t*-test implied that duplicates were not significantly different ($p>0.05$), the duplicates from the sampling periods 6 to 21 were regarded as repeated measures.

The result of one-way random effects model implied that the variability of octanol–water distribution coefficients at the fungal kingdom level stemmed from differences in the sampling period (Table 7). The one-way random effects model analyses for the three observations, i.e., all, hydrophobic ($\log_{10}D_{oct/wat}>0$), and hydrophilic ($\log_{10}D_{oct/wat}<0$) observations, were conducted separately and as a result, the sum of the squares of between sampling periods were larger than sum of the squares of within sampling period, indicating that the large variability originated from difference in the sampling period. In addition, at least one observation among total hydrophobic observations (N=27) was significantly different from the others ($p=0.004$). The octanol–water distribution coefficients during the sampling periods 6, 7, and 14 were significantly higher than those measured during other periods ($p<0.05$).

The Spearman's correlation analysis indicated a potential possibility that some environmental factors and taxon-specific relative abundance can affect the degree of octanol–water distribution coefficients (Table 8). The relative abundance of Dothideomycetes and Sordariomycetes across the sampling periods positively and

negatively correlated with the octanol–water distribution coefficients, respectively (p=0.017, p=0.032). The weekly concentrations of the anthropogenic pollutants, CO and NO_2, were negatively correlated with the octanol–water distribution coefficients (p=0.03, p=0.014, respectively).

The generalized linear model revealed that the octanol–water distribution coefficient at the kingdom level was affected by taxon-specific relative abundance, climatological condition, and weekly concentration of anthropogenic pollutants, and can exhibit large variation (Table 9). Among these variables, the concentrations of NO_3^- and NO_2 were highly responsible for the large variation in the octanol–water distribution coefficients. The type-III sum of squares, often referred to as the partial sums of squares, showed a proportion of variance that was influenced by each parameter. The type-III sum of squares for NO_3^- and NO_2 was 3.3 and 2.1, respectively, and was higher than other parameters. In addition, relative humidity, wind speed, and relative abundance of Sordariomycetes were considered important parameters, which can affect the octanol–water distribution coefficients at the fungal kingdom level.

Table 7. ANOVA table by one-way random effects model for variation of the octanol–water distribution coefficients at the kingdom level within and between sampling periods.

Observation	Source	Sum of Squares	Degrees of freedom	Mean squares	*F* value	*p*-value
All observations (N = 36)	Between sampling period	8.21	19	0.43	2.01	0.082
	Within sampling period	3.44	16	0.21	N.A	N.A
Hydrophobic observations (N=27) ($log_{10}D_{oct/wat}>0$)	Between sampling period	4.38	16	0.27	5.59	0.004
	Within sampling period	0.49	10	0.05	N.A	N.A
Hydrophilic observation (N=9) ($log_{10}D_{oct/wat}<0$)	Between sampling period	0.22	7	0.03	5.66	0.313
	Within sampling period	0.01	1	0.01	N.A	N.A

Table 8. Spearman's correlation analysis between the octanol–water distribution coefficients at the kingdom level and the variables that can affect the coefficients.

Variables		Number of observation	Spearman's correlation coefficients	p-value
Taxon-specific relative abundance[1]	Dothideomycetes	22	0.50	0.017
	Sordariomycetes	22	–0.46	0.032
	Leotiomycetes	22	0.41	0.060
	Eurotiomycetes	22	0.09	0.683
	Agaricomycetes	22	0.11	0.626
	Tremellomycetes	22	0.06	0.793
	Dacrymycetes	22	–0.10	0.660
	Microbotryomycetes	22	0.09	0.690
	Malasseziomycetes	22	–0.10	0.650
Climatological condition[2]	Precipitation[4] (mm)	27	–0.11	0.571
	Average relative humidity (%)	27	0.19	0.347
	Average temperature	27	0.14	0.475
	Wind speed (m/s)	27	0.08	0.678
Concentration of anthropogenic	SO_2 (ppm)	27	–0.15	0.452
	CO (ppm)	27	–0.42	0.030
	O_3 (ppm)	27	–0.30	0.124
	NO_2 (ppm)	27	–0.47	0.014
	PM_{10} ($\mu g/m^3$)	27	–0.35	0.077
	$PM_{2.5}$ ($\mu g/m^3$)	27	–0.03	0.889
	SO_4^{2-}	27	0.24	0.220
	NO_3^-	27	–0.25	0.218
	Cl^-	27	–0.03	0.865
	Na^+	27	0.07	0.721
	NH_4^+	27	0.14	0.484
	K^+	27	–0.43	0.026
	Mg^{2+}	27	0.23	0.240
	Ca^{2+}	27	0.11	0.583
	Organic carbon	27	–0.49	0.009
	Elemental carbon	27	–0.40	0.037

[1]Fungal class-specific relative abundance of each sampling period
[2]Data from the South Korea Meteorological Administration
[3]Data from the Ministry of Environment of South Korea
[4]Weekly total precipitation

Table 9. Final generalized linear model for the octanol–water distribution coefficient at the fungal kingdom level. Total sampling periods were regarded as random effects and were shown as intercept.

Parameter	Estimate	Standard error	Pr > |t|	Type III SS	Mean square	F Value	Pr > F
Intercept	17.5	3.2	0.0004				
Dothideomycetes	–4.6	1.6	<.0001	0.6	0.6	8.1	0.012
Sordariomycetes	–7.6	1.6	0.012	1.6	1.6	21.5	0.0003
Leotiomycetes	–9.5	3.3	0.0003	0.6	0.6	8.4	0.010
Agaricomycetes	–5.3	1.6	0.010	0.8	0.8	10.4	0.005
Tremellomycetes	–25.1	7.4	0.005	0.9	0.9	11.4	0.004
Dacrymycetes	–12.7	4.7	0.004	0.5	0.5	7.2	0.016
Relative humidity	–0.1	0.0	0.016	1.9	1.9	24.5	0.0001
Wind speed	–2.0	0.5	0.0001	1.5	1.5	20.2	0.0004
Temperature	0.1	0.02	0.0004	0.4	0.4	5.7	0.029
NO_2	–131.5	25.0	0.029	2.1	2.1	27.6	<.0001
NO_3^-	0.4	0.1	<.0001	3.3	3.3	42.8	<.0001

4. Discussion

The results obtained in this study revealed that octanol–water distribution coefficients of the fungal phyla, Ascomycota and Basidiomycota, varied on a weekly basis rather than have a distinct value (Figure 2). Ascomycota and Basidiomycota are regarded as the most abundant fungal phyla in the biosphere and atmosphere (Elbert et al., 2007). Consistent with this observation, in our study, the mean relative abundance of Ascomycota and Basidiomycota was 64.2% and 35.6%, respectively. We assumed that the octanol–water distribution coefficients of the two phyla will be significantly different because of their genetic differences. However, the paired *t*-test revealed that the octanol–water distribution coefficients of the two phyla were not significantly different.

The octanol–water distribution coefficients at the genus level were widely varied among genera (Table 5). Moreover, even though the fungal genera belonged to the same higher taxonomic level, the fungal genera were not taxonomically grouped according to the octanol–water distribution coefficients (Figure 2). This can be inferred from the fact that the hierarchical clustering method we used was based on the correlation of the octanol–water distribution coefficients observed in different genera. Therefore, if octanol–water distribution coefficients of different genera were observed in a similar pattern across the sampling period, then the cluster analysis involving different genera is expected to generate a highly similar cluster. This pattern seemingly stems from large variations in octanol–water distribution coefficients within each of the fungal genus across sampling periods (Table 5).

We speculated the possible reason for a large variation in the octanol–water distribution coefficients within each fungal genus is climatological conditions, such as temperature,

relative humidity and precipitation, and weekly concentration of anthropogenic pollutants such as gaseous and particulate air pollutants, which might modify the surface properties of fungal particles. The Spearman's correlation analysis implied that some environmental factors could likely affect the surface of fungal particles and change the degree of octanol–water distribution coefficients at the fungal kingdom level. The weekly concentrations of the anthropogenic pollutants, CO and NO_2, were negatively correlated with the octanol–water distribution coefficients (p=0.03, p=0.014, respectively). In addition, the linear mixed effect model revealed that the weekly concentration of NO_3^- and NO_2 could mainly modify the octanol–water distribution coefficients at the fungal kingdom level.

The modification of surface properties of fungal particles by gaseous and particulate air pollutants such as NO_2, O_3, diesel exhaust particles, and other nanoparticles may include protein nitration and an attachment. Under an optimal concentration of NO_2 and O_3 in the atmosphere, tyrosine present in airborne particles can transform into nitrotyrosine, thereby causing a shift in the pKa value of airborne particles (Franze et al., 2003, Abello et al., 2009 and Ackaert et al., 2014). Furthermore, fungal particles may undergo an alteration in their surface properties by reacting with other airborne particles (Deguillaume et al., 2008 and Després et al., 2012). Through the modification of surfaces of the fungal particle present in the atmosphere, the octanol–water distribution coefficients of the fungal particles might not be constant during the sampling period.

Several factors are associated with the chemical aging of fungal particles in the atmosphere, such as the aerodynamic diameter of fungal particles, metrological

condition, and concentration of air pollutants. However, we could not clearly elucidate a relationship between the chemical aging of fungal particles and the aforementioned factors because of the limitation of this study design. First, we could not measure the concentration of fungal particles that were derived from the original biosphere as well as that of chemically-aged fungal particles in the atmosphere. Second, we were not able to measure the size of each fungal particle and we could not estimate some other features of these fungal particles, such as deposition rate.

Although there are obvious limitations to this study, this research is important in the following aspects. With regard to public health, modification of the degree of hydrophobicity of fungal particles, which can act as IN or CCN, may influence the hydrological cycle and generate either positive or negative feedbacks to climatic change (Morris et al., 2014, Fröhlich-Nowoisky et al., 2016). Furthermore, to our knowledge, this is the first study to report the degree of hydrophobicity of fungal particles collected from the atmosphere, and to suggest a potential relationship between the degree of hydrophobicity of fungal particles and environmental factors, such as meteorological conditions and concentration of anthropogenic air pollutants. Thus, the results of this study can serve as the basic data for identifying the degree of hydrophobicity of fungal particles in the atmosphere.

5. Conclusion

Even though the limitation of this study obscures the exact reason for the large variation in the octanol–water distribution coefficients of fungal particles, the degree of hydrophobicity of fungal particles collected from the atmosphere in Seoul, South Korea, has been proposed in this study for the first time. The result of this study implied that the degree of hydrophobicity of fungal particles could vary depending on the species. In addition, the degree of hydrophobicity of fungal particles might be affected by ambient air pollutants, which seems to be influenced by concentration of the air pollutants and the residence time of fungal particles in the atmosphere. Consequently, we expect the ice- and cloud condensation-nucleation activity of fungal particles to vary depending on the fungal species and the residence time of the fungal particles in the atmosphere.

References

Abello, N., Kerstjens, H. A. M., Postma, D. S. and Bischoff, R. (2009) Protein Tyrosine Nitration: Selectivity, Physicochemical and Biological Consequences, Denitration, and Proteomics Methods for the Identification of Tyrosine-Nitrated Proteins, *Journal of Proteome Research*, **8**, 3222-3238.

Ackaert, C., Kofler S., Horejs-Hoeck, J., Zulehner, N., Asam, C., Grafenstein, S, Fuchs, J.E., Briza, P., Liedl, K.R., Bohle, B., Ferreira, F., Brandstetter, H., Oostingh, G.J. and Duschl, A. (2014) The impact of nitration on the structure and immunogenicity of the major birch pollen allergen Bet v 1.0101, *PloS one*, **9** (8), e104520.

Afgan, E., Baker, D., Beek, M., Blankenberg, D., Bouvier, D., Čech, M., Chilton, J., Clements, D., Coraor, N., Eberhard, C., Grüning, B., Guerler, A., Hillman-Jackson, J., Kuster, G., Rasche, E., Soranzo, N., Turaga, N., Taylor, J., Nekrutenko, A. and Goecks, J. (2016) The Galaxy platform for accessible, reproducible and collaborative biomedical analyses: 2016 update, *Nucleic Acids Research*, **44** (W1), W3-W10.

Altschul, S. F., Gish, W., Miller, W., Myers, E. W. and Lipman, D. J. (1990) Basic Local Alignment Search Tool, *Journal of Molecluar Biology*, **215**, 403-410.

An, C., Woo, C. and Yamamoto, N. (2017) Introducing DNA-based methods to compare fungal microbiota and concentrations in indoor, outdoor, and personal air, *Aerobiologia*, doi:http://doi.org/10.1007/s10453-017-9490-6.

An, C. and Yamamoto, N. (2016) Fungal compositions and diversities on indoor surfaces with visible mold growths in residential buildings in the Seoul Capital Area of South Korea, *Indoor Air*, **26** (5), 714-723.

Bolger, A. M., Lohse, M. and Usadel, B. (2014) Trimmomatic: a flexible trimmer for Illumina sequence data, *Bioinformatics*, **30** (15), 2114-2120.

Caporaso, J.G., Kuczynski, J., Stombaugh, J., Bittinger, K., Bushman, F.D., Costello, E.K., Fierer, N., Pena, A.G., Goodrich, J.K., Gordon, J.I., Huttley, G.A., Kelley, S.T., Knights, D., Koenig, J.E., Ley, R.E., Lozupone, C.A., Mcdonald, D., Muegge, B.D., Pirrung, M., Reeder, J.,

Sevinsky, J.R., Turnbaugh, P.J., Walters, W.A., Widmann, J., Yatsunenko, T., Zaneveld, J. and Knight, R. (2010) QIIME allows analysis of high-throughput community sequencing data, *Nature Methods*, **7**, 335-336.

Dannemiller, K. C., Lang-Yona, N., Yamamoto, N., Rudich, Y. and Peccia, J. (2014) Combining real-time PCR and next-generation DNA sequencing to provide quantitative comparisons of fungal aerosol populations, *Atmospheric Environment*, **84**, 113-121.

Dannemiller, K. C., Reeves, D., Bibby, K., Yamamoto, N. and Peccia, J. (2014) Fungal high-throughput taxonomic identification tool for use with next-generation sequencing (FHiTINGS), *Journal of Basic Microbiology*, **54** (4), 315-321.

Deguillaume, L., Leriche, M., Amato, P., Ariya, P. A., Delort, A. M., Pöschl, U., Chaumerliac, N., Bauer, H., Flossmann, A. and Morris, C. E. (2008) Microbiology and atmospheric processes: chemical interactions of Primary

Biological Aerosols, *Biogeosciences Discussions, European Geosciences Union*, **5** (1), 841-870.

Després, V. R., Huffman, J. A., Burrows, S. M., Hoose, C., Safatov, A. S., Buryak, G., Fröhlich-Nowoisky, J., Elbert, W., Andreae, M. O., Pöschl, U. and Jaenicke, R. (2012) Primary biological aerosol particles in the atmosphere: a review, *Tellus B: Chemical and Physical Meteorology*, **64** (1), 15598.

Elbert, W., Taylor, P. E., Andreae, M. O. and Pöschl, U. (2007) Contribution of fungi to primary biogenic aerosols in the atmosphere: wet and dry discharged spores, carbohydrates, and inorganic ions, *Atmospheric Chemistry and Physics*, **7** (17), 4569-4588.

Franze, T., Weller, M. G., Niessner, R. and Pöschl, U. (2005) Protein Nitration by Polluted Air, *Environmental Science & Technology*, **39**, 1673-1678.

Fröhlich-Nowoisky, J., Kampf, C. J., Weber, B., Huffman, J. A., Pöhlker, C., Andreae, M. O., Lang-Yona, N., Burrows, S. M., Gunthe, S. S., Elbert, W., Su, H., Hoor, P., Thines, E., Hoffmann, T., Després, V. R. and Pöschl, U. (2016) Bioaerosols in the Earth system: Climate, health, and ecosystem interactions, *Atmospheric Research*, **182**, 346-376.

Hassett, M. O., Fischer, M W. F. and Money, N. P. (2015) Mushrooms as Rainmakers: How Spores Act as Nuclei for Raindrops, *PloS one*, **10** (10), e0140407.

Hawksworth, D. L. (2001) The magnitude of fungal diversity: the 1.5 million species estimate revisited, *Mycological research*, **105** (12), 1422-1432.

Heald, C. L. and Spracklen, D. V. (2009) Atmospheric budget of primary biological aerosol particles from fungal spores, *Geophysical Research Letters*, **36** (9).

Hospodsky, D., Yamamoto, N. and Peccia, J. (2010) Accuracy, precision, and method detection limits of quantitative PCR for airborne bacteria and fungi, *Applied and Environmental Microbiology*, **76** (21), 7004-7012.

Iannone, R., Chernoff, D. I., Pringle, A., Martin. S. T. and Bertram, A. K. (2011) The ice nucleation ability of one of the most abundant types of fungal spores found in the atmosphere, *Atmospheric Chemistry and Physics*, **11** (3), 1191-1201.

Kumari, P., Woo, C., Yamamoto, N. and Choi, H. (2016) Variations in abundance, diversity and community composition of airborne fungi in swine houses across seasons, *Scientific Reports*, **6**, 37929.

Linder, M. B., Szilvay, G. R., Nakari-Setälä, T. and Penttilä, M, E. (2005) Hydrophobins: the protein-amphiphiles of filamentous fungi, *FEMS Microbiology Reviews*, **29** (5), 877-896.

Lindsley, W. G., Schmechel, D. and Chen, B. T. (2006) A two-stage cyclone using microcentrifuge tubes for personal bioaerosol sampling, *Journal of Environmental Monitoring*, **8** (11), 1136-1142.

Möhler, O., DeMott, P. J., Vali, G. and Levin, Z. (2007) Microbiology and atmospheric processes: the role of biological particles in cloud physics, *Biogeosciences*, **4**, 1059-1071.

Morris, C. E., Conen, F., Huffman, A., Phillips, V., Pöschl, U. and Sands, D. C. (2014) Bioprecipitation: a feedback cycle linking earth history, ecosystem dynamics and land use through biological ice nucleators in the atmosphere, *Global Change Biology*, **20** (2), 341-351.

Nilsson, R. H., Ryberg, M., Abarenkov, K., Sjökvist, E. and Kristiansson, E. (2009) The ITS region as a target for characterization of fungal communities using emerging sequencing technologies, *FEMS Microbiology Letter*, **296** (1), 97-101.

Sangster, J. (1989) Octanol-Water Partition Coefficients of Simple Organic Compounds, *Journal of Physical and Chemical Reference Data*, **18** (3), 1111-1227.

Schloss, P. D., Westcott, S. L., Ryabin, T., Hall, J. R., Hartmann, M., Hollister, E. B. Lesniewski, R. A., Oakley, B. B., Parks, D. H., Robinson, C. J., Sahl, J. W., Stres, B., Thallinger, G. G., Horn, D. J. V. and Weber, C. F. (2009) Introducing mothur: open-source, platform-independent, community-supported software for describing and comparing microbial communities, *Applied and Environmental Microbiolgy*, **75** (23), 7537-7541.

Schoch, C. L., Seifert, K. A., Huhndorf, S., Robert, V., Spouge, J. L., Levesque, C. A., Chen, W. and Fungal Barcoding Consortium (2012) Nuclear ribosomal internal transcribed spacer (ITS) region as a universal DNA barcode marker for Fungi, *Proceedings of the National Academy of Sciences USA*, **109** (16), 6241-6246.

Yamashita, T., Yamamoto, E. and Kushida, I. (2011) Frozen water phase method for log D measurement using a 96-well plate, *Talanta*, **84** (3), 809-813.

Yamamoto, N., Bibby, K., Qian, J., Hospodsky, D., Rismani-Yazdi, H., Nazaroff, W. W. and Peccia, J. (2012) Particle-size distributions and seasonal diversity of allergenic and pathogenic fungi in outdoor air, *ISME Journal*, **6** (10), 1801-18

Supporting information

Supplementary Table 1. Climatological conditions during the sampling periods. The data were obtained from the South Korea Meteorological Administration.

Sampling period ID	Sampling start day	Sampling start time	Sampling end day	Sampling end time	Temperature (℃)			Precipitation (mm)	RH* (%)	WS** (m s^{-1})
					Highest	Average	Lowest		Average	Average
1	160614	16:13	160621	16:13	28.7	23.6	19.4	15.5	66.2	2.2
2	160621	16:30	160628	16:30	29.1	24.3	20.2	34.1	65.0	2.1
3	160628	16:50	160705	16:50	27.1	23.8	21.1	242.7	76.8	2.4
4	160705	17:00	160712	17:00	30.3	26.0	21.9	103.5	71.0	1.9
5	160712	17:15	160719	17:15	28.7	25.0	21.9	53.8	72.2	2.3
6	160719	17:30	160726	7:30	32.1	28.3	25.2	1.0	68.2	2.0
7	160726	18:30	160802	18:30	31.1	27.9	25.8	62.9	73.6	2.1
8	160802	19:00	160809	18:00	34.4	29.9	26.0	3.0	63.7	1.7
9	160809	18:30	160816	19:00	34.6	29.6	26.4	1.7	67.4	2.0
10	160816	19:30	160823	19:30	34.7	29.7	26.2	20.4	62.5	1.8
11	160823	20:00	160830	20:00	29.0	24.3	20.8	34.0	59.5	2.6
12	160831	10:30	160907	12:30	28.0	23.8	20.0	22.5	71.9	2.3
13	160907	13:00	160914	14:00	28.6	24.1	20.8	7.0	68.3	1.7
14	160914	14:30	160921	14:30	28.0	22.8	18.4	7.0	56.9	2.4
15	160921	15:00	160928	16:00	26.7	21.7	17.6	14.0	61.5	1.6
16	160928	16:30	161005	16:30	25.3	20.8	17.7	25.5	70.4	2.2
17	161005	17:00	161012	17:00	22.1	16.5	11.7	8.0	58.1	2.4
18	161012	17:30	161019	17:30	22.8	17.0	12.3	1.5	64.0	1.5
19	161020	9:00	161027	9:30	20.5	15.7	11.8	39.5	66.3	2.3

20	161027	13:30	161103	13:30	13.1	8.2	3.0	1.1	52.4	2.1
21	161103	14:00	161108	13:00	15.4	11.2	7.6	6.2	66.0	2.7

*Relative humidity
**Wind speed

Supplementary Table 2. Weekly concentrations of anthropogenic air pollutants. The data were obtained from the Ministry of Environment of South Korea.

Sampling period ID	SO_2* (ppm)	CO* (ppm)	O_3* (ppm)	NO_2* (ppm)	$PM_{2.5}$** (μg/m^3)	PM_{10}** (μg/m^3)	SO_4^{2-}**	NO_3^-**	Cl^-**	Na^+**	NH_4^+**	K^+**	Mg^{2+}**	Ca^{2+}**	OC**	EC**
1	0.01	0.51	0.05	0.03	32.5	42.0	7.8	4.8	0.12	0.04	4.5	0.27	0.06	0.25	3.2	1.1
2	0.01	0.50	0.04	0.03	32.7	41.9	5.7	5.4	0.08	0.01	3.7	0.27	0.06	0.17	4.5	1.3
3	0.00	0.38	0.03	0.02	18.7	23.6	4.9	1.9	0.05	0.00	2.3	0.07	0.05	0.18	2.0	0.8
4	0.01	0.48	0.03	0.03	29.0	35.6	5.1	3.4	0.06	0.00	2.7	0.03	0.09	0.21	4.1	1.9
5	0.01	0.40	0.02	0.03	12.9	16.8	2.2	0.8	0.04	0.01	1.1	0.01	0.00	0.09	1.7	0.5
6	0.01	0.42	0.03	0.02	23.3	28.4	5.6	1.0	0.06	0.07	2.3	0.01	0.01	0.07	3.1	0.8
7	0.00	0.38	0.02	0.02	20.9	26.3	7.6	1.5	0.09	0.09	3.2	0.06	0.03	0.13	2.2	0.7
8	0.01	0.44	0.04	0.03	18.4	24.5	4.1	0.8	0.02	0.05	1.8	0.16	0.00	0.02	4.2	1.0
9	0.01	0.39	0.03	0.03	19.7	23.2	7.3	2.1	0.05	0.13	2.9	0.09	0.01	0.00	2.7	0.9
10	0.01	0.44	0.04	0.03	19.9	26.7	4.4	1.1	0.04	0.11	1.4	0.08	0.00	0.02	4.5	1.1
11	0.01	0.29	0.03	0.02	8.7	12.4	1.2	0.3	0.03	0.09	0.4	0.09	0.01	0.05	1.4	0.5
12	0.01	0.48	0.04	0.03	21.6	28.5	6.2	2.1	0.09	0.11	2.6	0.14	0.02	0.06	2.6	1.1
13	0.01	0.52	0.03	0.04	22.8	28.7	6.5	2.5	0.03	0.06	2.9	0.10	0.01	0.04	2.5	1.2
14	0.01	0.36	0.04	0.02	18.5	22.8	4.9	1.6	0.03	0.09	2.1	0.08	0.01	0.10	2.4	0.7
15	0.01	0.54	0.03	0.05	28.7	35.8	3.7	2.9	0.06	0.07	2.1	0.08	0.01	0.09	6.1	1.3
16	0.01	0.45	0.02	0.03	19.7	24.0	3.0	3.2	0.08	0.07	1.9	0.06	0.01	0.08	2.6	1.1
17	0.01	0.46	0.03	0.03	18.5	30.0	2.1	2.1	0.10	0.03	1.2	0.14	0.01	0.09	3.1	0.8
18	0.01	0.74	0.02	0.05	36.8	57.2	7.3	6.0	0.14	0.01	4.0	0.24	0.01	0.17	4.9	1.9
19	0.01	0.50	0.02	0.03	17.7	32.0	2.7	2.2	0.12	0.02	1.3	0.14	0.01	0.14	2.9	0.9
20	0.01	0.47	0.02	0.04	17.6	33.0	1.4	2.3	0.20	0.03	1.0	0.11	0.01	0.10	3.0	0.9
21	0.01	0.55	0.03	0.03	34.3	54.8	5.5	6.7	0.63	0.14	4.6	0.27	0.03	0.13	5.5	1.4

*Data from Gwankak-gu station

**Data from Eunpyeong-gu station

Supplementary Table 3. Numbers and mean lengths of filtered high-quality reads derived by 2 × 300 bp sequencing by Illumina MiSeq.

Sampling period ID	Sample ID	Duplicate	Octanol		Water	
			Number of sequence	Mean sequence length (bp)	Number of sequence	Mean sequence length (bp)
1	OW1D1	1	23465	305	117858	301
2	OW2D1	1	65664	303	57592	307
4	OW4D1	1	73856	304	6197	305
5	OW5D1	1	66879	290	51412	293
6	OW6D1	1	N.A	N.A	N.A	N.A
6	OW6D2	2	N.A	N.A	N.A	N.A
7	OW7D1	1	6902	300	18268	313
	OW7D2	2	66219	306	16955	320
8	OW8D1	1	N.A	N.A	58645	305
	OW8D2	2	74344	316	23787	311
9	OW9D1	1	N.A	N.A	N.A	N.A
	OW9D2	2	N.A	N.A	N.A	N.A
10	OW10D1	1	66628	298	3134	281
	OW10D2	2	N.A	N.A	39472	302
11	OW11D1	1	73399	294	16379	293
	OW11D2	2	70683	285	69471	290
12	OW12D1	1	68982	291	81931	292
	OW12D2	2	65046	288	51798	295
13	OW13D1	1	11966	280	20585	290
	OW13D2	2	38239	290	55235	329
14	OW14D1	1	N.A	N.A	59620	308
	OW14D2	2	82162	306	34	260
15	OW15D1	1	104586	314	64899	311
	OW15D2	2	19419	315	85689	305
16	OW16D1	1	46146	292	86243	314
	OW16D2	2	79102	294	4967	292
17	OW17D1	1	98788	280	42465	286
	OW17D2	2	96087	278	79220	287
18	OW18D1	1	25595	331	24141	280
	OW18D2	2	75405	308	69057	298
19	OW19D1	1	1680	288	48561	298
	OW19D2	2	81001	303	80873	299
20	OW20D1	1	90653	286	89941	286
	OW20D2	2	11054	277	87641	289
21	OW21D1	1	7957	298	59123	291
	OW21D2	2	25796	284	56207	289

국문초록

대기 중 부유 진균의 옥탄올–물 분배계수 연구

우철운

환경보건학과 환경보건학 전공

서울대학교 보건대학원

포자를 이용하여 번식하는 진균은 그 종에 따라 형태, 크기, 표면 특성과 같은 다양한 특성을 가진 포자를 생산하여 서로 다른 환경에 적응하여 온 생물이다. 최근, 포자 혹은 균사와 같은 부유 진균 입자들이 대기 중에서 얼음 핵 또는 구름 응결핵으로 작용할 수 있고 지역적 혹은 전지구적인 물의 순환에 한 축으로서 참여할 수 있는 것이 제기되고 있다.

이와 같은 진균의 역할에 있어, 진균 입자 표면의 소수성 정도는 얼음 핵 또는 구름 응결핵으로 작용하는 현상에 중요한 역할을 할 것이라 여겨졌다. 따라서, 이 연구에서는 옥탄올-물 분배계수를 사용하여 서울의 대기 중에서 모아진 진균 입자 표면의 소수성 정도를 확인하는 것을 목표로 하였다. 대기 중의 부유 진균 입자는 two-stage cyclone sampler 를 사용하여 채취되었다. 채취된 진균 입자는 frozen water phase method 를 사용하여 진균 입자 개개의 표면 특성에 따라 옥탄올과 물에 각각 나뉘어졌다. 진균 분류군 특이적 옥탄올-물 분배계수는 quantitative PCR 과 high-throughput sequencing 에 의해 산출되었다. 진균의 주요 문 (phylum level) 인 Ascomycota 와 Basidiomycota 의 옥탄올–물 분배계수는 통계적으로 큰 차이가 없었다 ($p>0.05$). 또한, Ascomycota 와 Basidiomycota 의 옥탄올–물 분배계수는 채취 기간에 따라 비슷한 변동을 보였다. 진균 속 (genus level) 에서의 옥탄올–물 분배계수는 채취 기간 동안 매우 큰 변동을 보였다. 진균 속의 옥탄올–물 분배계수에 근거한 위계적 군집 분석의 결과는 진균의 속이 옥탄올–물 분배계수에 의해 분류학적인 군집이 이루어지지 않음을 보였다. Spearman’s

correlation analysis 와 generalized linear model 을 통해 진균 입자의 표면 특성이 기상학적 조건과 대기오염물질의 농도에 영향을 받아 옥탄올–물 분배계수가 달라질 수 있음을 확인하였다. 이 연구의 결과는 진균 입자의 소수성 정도가 같은 상위 분류군에 속하는 진균의 종이라 하더라도 각각 다를 수 있음을 의미한다. 또한, 진균 입자의 소수성 정도가 대기오염물질에 의해 영향을 받았을 수 있고, 이것은 대기오염물질의 농도 및 진균 입자의 대기 중 체류 시간에 따라 달라질 수 있는 것으로 생각된다. 따라서, 얼음 핵 또는 구름 응결핵으로 작용할 수 있는 진균 입자의 능력은 진균 종에 따라 혹은 진균 입자의 대기 중 체류 시간에 따라 달라질 수 있다.

주요어: 옥탄올–물 분배계수, 대기 중 부유 진균 입자, 표면 특성, 소수성 정도, 얼음핵, 구름응결핵

학번: 2016-24051